Trends in
Statistical Physics
Vol. 3, (2000)

Nonlinear Couette flow in dilute gases

José M. Montanero [a] and Vicente Garzó [b]

[a] Departamento de Electrónica e Ingeniería Electromecánica, Universidad de Extremadura, E-06071 Badajoz, Spain. [b] Departamento de Física, Universidad de Extremadura, E-06071, Badajoz, Spain

ABSTRACT

An overview of recent work on nonlinear Couette flow in a dilute gas is presented. The analysis is made within the framework of the Boltzmann equation by following three different and complementary routes: (i) the application of the Grad method to the Boltzmann equation, (ii) the analytical solutions of the BGK and ellipsoidal statistical (ES) models, and (iii) the use of the Direct Simulation Monte Carlo (DSMC) method to numerically solve the true Boltzmann equation. In the bulk domain, we found a solution characterized by constant pressure, and linear velocity and parabolic temperature profiles with respect to a scaled variable. The main transport coefficients of the problem are obtained as nonlinear functions of the reduced shear rate. The predictions of the kinetic models and those obtained by using the Grad method are compared with both molecular dynamics and Monte Carlo simulations. The comparison shows that the results derived from the kinetic models present a better agreement with the computer simulations than those obtained from the Grad method, especially in the case of the ES model.

1 INTRODUCTION

The steady planar Couette flow is one of the most interesting states to analyze transport phenomena. The physical situation corresponds to a fluid enclosed between two infinite parallel plates in relative motion and, in general, kept at different temperatures. These boundary conditions lead to combined heat and momentum transport across the system. Let x and y be the coordinates parallel to the flow and orthogonal to the plates, respectively. In the steady state, the corresponding hydrodynamic balance equations are

$$\frac{\partial P_{xy}}{\partial y} = \frac{\partial P_{yy}}{\partial y} = 0, \tag{1}$$

$$P_{xy}\frac{\partial u_x}{\partial y} + \frac{\partial q_y}{\partial y} = 0, \tag{2}$$

where $\mathbf{u} = u_x\widehat{\mathbf{x}}$ is the flow velocity, P is the pressure tensor, and $\mathbf{q} = q_x\widehat{\mathbf{x}} + q_y\widehat{\mathbf{y}}$ is the heat flux. Equation (2) shows that a thermal gradient $\partial T/\partial y$ is present due to the nonzero velocity gradient, even if both plates are at the same temperature. In addition, Eqs. (1) and (2) do not constitute a closed set unless one knows the dependence of the pressure tensor and the heat flux on the hydrodynamic fields. Thus, if the strength of the gradients is small, the fluxes P and $\mathbf{q}$ are correctly given by the Navier-Stokes (NS) constitutive relations, which in this problem yield

$$P_{xx} = P_{yy} = P_{zz}, \quad P_{xy} = -\eta_0\frac{\partial u_x}{\partial y}, \tag{3}$$

$$q_x = 0, \quad q_y = -\kappa_0\frac{\partial T}{\partial y}, \tag{4}$$

where η_0 and κ_0 are the NS shear viscosity and thermal conductivity coefficients, respectively. According to Eqs. (1) and (3) the hydrostatic pressure $p = [P_{xx} + P_{yy} + (d-2)P_{zz}]/d$ is a constant, where d represents the dimensionality of the system ($d = 2$ or $d = 3$).

Even in the NS regime, the Couette flow problem can be only exactly solved when one knows the spatial dependence of the transport coefficients. One possibility is to consider a dilute gas for which the state of the system is completely determined by the velocity distribution function, $f(\mathbf{r}, \mathbf{v}; t)$ satisfying the Boltzmann equation (BE) [1]. A solution of the BE can be obtained by means of the Chapman-Enskog method [2] as an expansion of the

distribution function in terms of the Knudsen number Kn=λ/ℓ_h, λ and ℓ_h being the mean free path and the scale length of the hydrodynamic gradients, respectively. The results indicate that the ratio η_0/κ_0 is a constant, so that Eqs. (1)–(4) lead to

$$\eta_0 \frac{\partial u_x}{\partial y} = \text{const}, \tag{5}$$

$$\left(\kappa_0 \frac{\partial}{\partial y}\right)^2 T = -\frac{\kappa_0}{\eta_0}\left(\eta_0 \frac{\partial u_x}{\partial y}\right)^2 = \text{const}. \tag{6}$$

Equation (5) shows that the velocity profile is not strictly linear since η_0 depends on y through the temperature. In the same way as u_x, the temperature profile is not strictly parabolic. As a matter of fact, the specific form of both hydrodynamic profiles depend on the interaction potential considered.

Our main goal is to get the hydrodynamic profiles and the transport properties for arbitrary values of the shear rate and the thermal gradient. In this regime, the linear NS relationships are not valid and the transport must be described by *nonlinear* constitutive equations. In the context of the BE, Tij and Santos [3] have shown that the BE admits a consistent solution in the nonlinear Couette problem for gas of Maxwell molecules (particles interacting via an r^{-4} potential). This solution is characterized by a constant pressure p and similar profiles as those of the linear regime, but replacing in (5) and (6) the transport coefficients η_0 and κ_0 by a generalized shear viscosity η and a generalized thermal conductivity κ_{yy}, respectively. However, these functions may not be explicitly obtained since it involves the infinite hierarchy of moment equations which cannot be recursively solved. For this reason, Tij and Santos [3] used a perturbation expansion in powers of the shear rate up to the super-Burnett approximation. Therefore, if one is interested in getting the full shear rate dependence of the transport coefficients, either one performs computer simulations or on the analytical side one considers alternative approximate methods.

A well-known technique of solving the BE is the Grad moment expansion method [4]. By using it, Risso and Cordero [4] have explicitly evaluated η and κ_{yy} for $d = 2$ and $d = 3$. When the physical quantities are conveniently scaled, their results are valid for general interaction potentials. Beyond the NS regime, they found that these coefficients turn out to be highly nonlinear functions of the shear rate. On the other hand, the use of kinetic models [5]–[9] can be also considered as another reliable tool to analyze transport phenomena. In this context, explicit expressions for the nonlinear transport coefficients of the Couette flow problem have been obtained from exact solutions of the Bhatnagar-Gross-Krook (BGK) [5, 6] and ellipsoidal statistical (ES) [7]–[9] models. The results also apply for general interaction potentials.

As a complementary alternative to analytical methods, one can get *semiexperimental* results from microscopic computational techniques by using molecular dynamics (MD) or Monte Carlo simulations. In order to validate their analytical predictions, Risso and Cordero [4] have also performed MD simulations of a hard disk gas to compute the shear rate dependence of the transport coefficients. Comparison between the results derived from the different theories with those obtained from simulations shows that in general, the results given by the kinetic models are in better agreement than those given by the Grad method[9]. Nevertheless, the above comparison is restricted to values of shear rates for which non-Newtonian effects are not quite significant. This is basically due to the difficulties inherent to MD simulations to achieve large shear rates. A possible way to overcome such problem and extend the range of values of shear rates is to use the so-called Direct Simulation Monte Carlo (DSMC) method [10]. This method has been shown in the past few years as an efficient algorithm to numerically solve the BE. Very recently, the DSMC method has been applied to the BE in the steady planar Couette flow in the cases of Maxwell molecules and hard spheres [11]. Since our interest lies on describing transport in the bulk domain (far away from the boundaries), new nonequilibrium boundary conditions based on the solution of the BGK model for the Couette flow have been employed to diminish the influence of the finite size effects.

In this paper we present a short review of recent work on nonlinear Couette flow in a dilute gas. The plan of the paper is as follows. In Sec. II we give a brief description of the planar Couette flow. A summary of the main analytical results obtained from the BE and from the kinetic models is given in Sec. III. In Sec. IV we offer a comparison between the different theoretical predictions and those obtained from MD simulations for hard disks. Section V is mainly devoted to introduce the boundary conditions in the DSMC simulations while in Sec. VI we compare all the analytical results with those given by the Monte Carlo simulations. The paper is closed in Sec. VII with some concluding remarks.

2 DESCRIPTION OF THE PROBLEM

For a dilute gas, the state of the system is completely specified through the one-particle velocity distribution function $f(\mathbf{r}, \mathbf{v}; t)$. This distribution function obeys the nonlinear BE, which in the absence of external forces

reads [1]

$$\frac{\partial f}{\partial t} + \mathbf{v}\cdot\nabla f = J[f,f], \tag{7}$$

where

$$J[f,f] = \int d\mathbf{v}_1 \int d\hat{\mathbf{k}}\, g I(g,\hat{\mathbf{k}}) \left[f(\mathbf{v}')f(\mathbf{v}_1') - f(\mathbf{v})f(\mathbf{v}_1)\right] \tag{8}$$

is the collision operator. In this equation, $I(g,\hat{\mathbf{k}})$ is the differential cross section, $g \equiv |\mathbf{v}-\mathbf{v}_1|$ being the relative velocity, and $(\mathbf{v}',\mathbf{v}_1')$ are precollisional velocities yielding postcollisional velocities $(\mathbf{v},\mathbf{v}_1)$. From the distribution function, one may define the local number density

$$n = \int d\mathbf{v}\, f, \tag{9}$$

the local flow velocity

$$\mathbf{u} = \frac{1}{n}\int d\mathbf{v}\,\mathbf{v}\, f, \tag{10}$$

the local temperature

$$T = \frac{m}{dnk_B}\int d\mathbf{v}\,\mathbf{V}^2 f, \tag{11}$$

the pressure tensor

$$\mathsf{P} = m\int d\mathbf{v}\,\mathbf{V}\mathbf{V} f, \tag{12}$$

and the heat flux

$$\mathbf{q} = \frac{m}{2}\int d\mathbf{v}\,\mathbf{V}^2\mathbf{V} f. \tag{13}$$

In the above expressions, m is the mass of a particle, k_B is the Boltzmann constant and $\mathbf{V} = \mathbf{v}-\mathbf{u}$ is the peculiar velocity. In addition, the equation of state is $p = nk_BT$.

The NS transport coefficients η_0 and κ_0 as obtained from the Chapman-Enskog method in the first Sonine approximation are [2]

$$\eta_0 = \frac{p}{\nu}, \quad \kappa_0 = \frac{d+2}{2}\frac{k_B}{m\mathrm{Pr}}\eta_0, \tag{14}$$

where $\nu = \theta n$, θ being an eigenvalue of the linearized Boltzmann collision operator [12]. Here, Pr is the Prandtl number, which in the first Sonine approximation is Pr=1−$1/d$. For the special case of Maxwell molecules (3D-particles interacting via an r^{-4} potential), the expressions (14) and the above formula for the Prandtl number are exact [2].

As said in the Introduction, we want to study the planar Couette flow for a dilute gas. We consider a gas enclosed between two parallel plates in relative motion and maintained at different temperatures. In the steady state, the BE becomes

$$v_y\frac{\partial}{\partial y}f = J[f,f], \tag{15}$$

where we have taken the gradients along the y direction. In principle, this equation must be solved together with specific boundary conditions. Nevertheless, we are interested in describing the state of the gas in the hydrodynamic regime, namely, for times much longer than the mean free time and for distances from the boundaries much larger than the mean free path. The main feature of this "normal" solution is that all the space dependence of f is given through the local density, the local velocity, the local temperature and their gradients. In the particular case of Maxwell molecules, Eq. (15) admits an exact normal solution [3] characterized by the following hydrodynamic profiles:

$$p = \text{const}, \tag{16}$$

$$\frac{1}{\nu(y)}\frac{\partial u_x}{\partial y} \equiv a = \text{const}, \tag{17}$$

$$\left[\frac{1}{\nu(y)}\frac{\partial}{\partial y}\right]^2 T = -\mathrm{Pr}\frac{2m}{k_B}\gamma(a). \tag{18}$$

These profiles can be seen as simple generalizations of those predicted by the NS approximation, Eqs. (5) and (6). The dimensionless parameter $\gamma(a)$ is a measure of the temperature profile curvature, and its value depends on the reduced shear rate a. In the limit $a \to 0$, the curvature $\gamma(a)$ behaves as $\gamma \approx a^2/5$. In addition, the pressure tensor does not depend on the thermal gradient and the heat flux is proportional to the (local) thermal gradient (generalized Fourier's law).

Since all the fluxes are nonlinear functions of the reduced shear rate a, it is convenient to introduce generalized transport coefficients characterizing the nonlinear response of the system. First, the fluxes P_{xy} and q_y can be written as

$$P_{xy} = -\eta(a)\frac{\partial u_x}{\partial y} \equiv -\eta_0 F_\eta(a)\frac{\partial u_x}{\partial y}, \tag{19}$$

$$q_y = -\kappa_{yy}(a)\frac{\partial T}{\partial y} \equiv -\kappa_0 F_\kappa(a)\frac{\partial T}{\partial y}, \tag{20}$$

where $\eta(a)$ and $\kappa_{yy}(a)$ are the generalized shear viscosity and the generalized thermal conductivity, respectively. The dimensionless viscosity function $F_\eta(a)$ and the thermal conductivity function $F_\kappa(a)$ are the most relevant quantities of the problem. The curvature $\gamma(a)$ can be expressed in terms of $F_\eta(a)$ and $F_\kappa(a)$ as $\gamma(a) = a^2F_\eta(a)/5F_\kappa(a)$. A curious non-Newtonian effect is the existence of a (nonzero) component of the heat flux orthogonal to the thermal gradient. This flux can be characterized by

a new generalized transport coefficient $\kappa_{xy}(a)$ defined as

$$q_x = -\kappa_{xy}(a)\frac{\partial}{\partial y}T \equiv -\kappa_0\Phi(a)a\frac{\partial}{\partial y}T. \tag{21}$$

The function $\Phi(a)$ is a generalization of a Burnett coefficient. In fact, $\Phi(0) = -7/2$ for Maxwell molecules and for hard spheres in the first Sonine approximation [2]. Normal stress differences are different from zero and are measured by the viscometric functions. However, since no MD simulation data for these elements have been reported, we have considered here more convenient to focus our attention on the study of F_η, F_κ and Φ.

3 ANALYTICAL RESULTS

3.1 Perturbative solution of the BE for Maxwell molecules

As said above, an exact solution of the BE has been found in the nonlinear Couette flow state for Maxwell molecules. Nevertheless, in order to calculate the full nonlinear dependence of F_η, F_κ and Φ on a one has to deal with an infinite hierarchy. This hierarchy can only be solved step by step by performing a perturbation expansion in powers of the shear rate. Tij and Santos [3] have computed the solution up to super-Burnett order. The result is

$$F_\eta(a) = 1 - 3.111a^2 + \mathcal{O}(a^4), \tag{22}$$

$$F_\kappa(a) = 1 - 7.259a^2 + \mathcal{O}(a^4). \tag{23}$$

The limitation of these results is evident since on the one hand, they are restricted to Maxwell molecules and on the other hand, they are not useful when the shear rate is not small. Consequently, one has to consider alternative approximate schemes, such as the application of the Grad method to the BE and/or the use of kinetic models. In both approaches, one looks for a solution having the same hydrodynamic profiles as in the case of the BE for Maxwell molecules, cf. Eqs. (16)–(18). This solution describes the transport in the hydrodynamic regime and so, it is insensitive to the details of the boundary conditions. Furthermore, since the reduced shear rate is defined as in Eq. (17) with $\nu = p/\eta_0$, the results obtained from Grad's method [4] and from the kinetic models [8] are *universal*, namely, the functions $F_\eta(a)$, $F_\kappa(a)$, and $\Phi(a)$ do not depend on the interaction potential.

3.2 Grad's method as applied to the BE

In the thirteen-moment Grad method the actual distribution function is replaced by [4]

$$f \to f_L\left\{1 + \frac{m}{n(k_BT)^2}\left[\left(\frac{mV^2}{5k_BT} - 1\right)\mathbf{V}\cdot\mathbf{q} + \tfrac{1}{2}\left(P_{ij} - p\delta_{ij}\right)V_iV_j\right]\right\}, \tag{24}$$

where

$$f_L = n\left(\frac{m}{2\pi k_BT}\right)^{3/2}\exp\left(-\frac{mV^2}{2k_BT}\right). \tag{25}$$

is the local equilibrium distribution function. From the approximation (24), a closed set of equations for n, $\mathbf{u}$, P, and $\mathbf{q}$ is derived when one takes velocity moments in the BE (7). Taking into account the planar Couette flow geometry, it can be seen that there are only eight independent moments, instead of the original thirteen moments appearing in Eq. (24). When the nonlinear terms in the fluxes are neglected, the set of independent moment equations admits a solution consistent with the profiles (16)–(18). In Ref. [4], explicit expressions for the generalized transport coefficients F_η, F_κ, and Φ were obtained as nonlinear functions of the reduced shear rate a. In the case of $d = 2$, their expressions are

$$F_\eta(a) = \frac{8}{4 + 15a^2 + \Delta(a)}, \tag{26}$$

$$F_\kappa(a) = \frac{15a^2 - \Delta(a) - 12}{4(1 - 3a^2)(3a^2 - 4)}, \tag{27}$$

$$\Phi(a) = \frac{8 - 54a^2 + 27a^4 + (3a^2 - 2)\Delta(a)}{4a^2(3a^2 - 1)(3a^2 - 4)}, \tag{28}$$

where $\Delta(a) \equiv \sqrt{16 + 120a^2 - 63a^3}$. For small shear rates, the above transport coefficients behave as $F_\eta \simeq 1 - \frac{15}{4}a^2$, $F_\kappa \simeq 1 + \frac{9}{4}a^2$ and $\Phi \simeq -\frac{9}{2}(1 + \frac{1}{4}a^2)$. The corresponding expressions for $d = 3$ are

$$F_\eta(a) = \frac{2}{1 + \frac{72}{25}a^2 + \Delta'(a)}, \tag{29}$$

$$F_\kappa(a) = \frac{4}{1 - \frac{216}{25}a^2 + 3\Delta'(a)}, \tag{30}$$

$$\Phi(a) = -7\frac{1 - \frac{36}{125}a^2}{1 + \frac{6}{5}a^2 + (1 - \frac{63}{25}a^2)\Delta'(a)}, \tag{31}$$

where $\Delta'(a) \equiv \sqrt{1 + \frac{116}{25}a^2 - \frac{864}{625}a^4}$. For small shear rates, the above transport coefficients behave as $F_\eta \simeq 1 - \frac{13}{5}a^2$, $F_\kappa \simeq 1 + \frac{21}{50}a^2$, and $\Phi \simeq -\frac{7}{2}(1 - \frac{197}{250}a^2)$. As said before, all these results are independent of the interaction potential.

3.3 Kinetic models of the BE

A kinetic model is constructed by replacing the complicated Boltzmann collision operator $J[f,f]$ by a simpler collision term which retains the qualitative and average properties of the true $J[f,f]$. In the case of the ES model, one replaces $J[f,f]$ by [1]

$$J[f,f] \to -\zeta(f - f_R), \tag{32}$$

where ζ is an effective collision frequency which can depend on the density and temperature, and

$$f_R(\mathrm{v}) = n\pi^{-d/2}(\det \Lambda)^{1/2}\exp(-\Lambda_{ij}V_iV_j). \tag{33}$$

Here, $\Lambda = [A\mathsf{I} - (B/mn)\mathsf{P}]^{-1}$, $A = (2k_BT/m)\mathrm{Pr}^{-1}$, I is the unit tensor, and $B = 2(\mathrm{Pr}^{-1} - 1)$. The Prandtl number Pr plays here the role of an extra parameter. If one takes Pr=1, f_R reduces to the local Maxwellian and the ES model reduces to the well-known BGK equation [1]. Consequently, the ES model can be seen as an extension of the simple BGK model to account for the correct Prandtl number Pr= $1-1/d$. This can be particularly important in situations where combined heat and momentum transport occurs, as it is the case of steady Couette flow. In the ES model, it is straightforward to evaluate the NS transport coefficients, namely, the shear viscosity coefficient η_0 and the thermal conductivity coefficient κ_0. The result is $\eta_0 = p/(\zeta\mathrm{Pr}^{-1})$ and $\kappa_0 = (d+2)pk_B/2m\zeta$. Thus, if we identify ζ as $\zeta\mathrm{Pr}^{-1} = \nu$ and take $\mathrm{Pr} = 1-1/d$, then the ES expressions of the transport coefficients coincide with those derived from the BE in the first Sonine approximation. Here, ν is the collision frequency appearing in Eqs. (14).

In the nonlinear Couette flow problem, it is convenient to express the generalized transport coefficients of the ES model in terms of an auxiliary parameter β, defined as the solution of the implicit equation [8, 9]

$$\begin{aligned} a^2 &= \beta[\mathrm{Pr}(\mathrm{Pr}+\overline{\mathrm{Pr}}C_1)]^2\,[2F_2 + dF_1(\mathrm{Pr}+\overline{\mathrm{Pr}}C_1)] \\ &\quad\times[\mathrm{Pr}(F_0^2\overline{\mathrm{Pr}} + F_1\mathrm{Pr}) + \overline{\mathrm{Pr}}C_1(F_0^2\overline{\mathrm{Pr}} + 2F_1\mathrm{Pr}) \\ &\quad + C_1^2F_1\overline{\mathrm{Pr}}^2 - 2\beta F_0^2F_2\overline{\mathrm{Pr}}^2]^{-1}, \end{aligned} \tag{34}$$

where $\overline{\mathrm{Pr}} = \mathrm{Pr} - 1$,

$$C_1(\beta) = 2\beta(F_1 + 2F_2) - 1, \tag{35}$$

and $F_r(\beta) = [(d/d\beta)\beta]^r F_0(\beta)$,

$$F_0(\beta) = \frac{2}{\beta}\int_0^\infty dt\, t\, e^{-t^2/2}K_0(2\beta^{-1/4}t^{1/2}), \tag{36}$$

K_0 being the zeroth-order modified Bessel function. The function $\gamma(a)$ is given by

$$\gamma = [1 + \overline{\mathrm{Pr}}(1 + C_1)]\,\mathrm{Pr}^2\beta\,. \tag{37}$$

The generalized transport coefficients are

$$F_\eta = \frac{\mathrm{Pr}^2F_0}{(\mathrm{Pr}+\overline{\mathrm{Pr}}C_1)^2}\,, \tag{38}$$

$$F_\kappa = \frac{\mathrm{Pr}}{2+d}\frac{a^2}{\gamma}F_\eta, \tag{39}$$

$$\begin{aligned} \Phi &= -\frac{\mathrm{Pr}^{-3}C_4}{a(2+d)}\{4a^3C_4(F_2 + 5F_3 + 8F_4 + 4F_5) \\ &\quad + 6\mathrm{Pr}\,a^2C_4C_6(F_2 + 4F_3 + 4F_4) + \mathrm{Pr}^2a[6C_3F_2 \\ &\quad + C_4(F_2 + 2F_3)(2 + 3C_6^2) + 2(d-2)C_5F_2] \\ &\quad + \mathrm{Pr}^3C_6[3C_3F_1 + C_4(F_1 + 2F_2)(1 + C_6^2) \\ &\quad + (d-2)C_5F_1]\}. \end{aligned} \tag{40}$$

In the above equations,

$$C_2(\beta) = 2\beta F_1 - 1, \tag{41}$$

$$\begin{aligned} C_3(\beta) &= \frac{1}{(\mathrm{Pr}+\overline{\mathrm{Pr}}C_1)^3(\mathrm{Pr}+\overline{\mathrm{Pr}}C_2)}\{(\overline{\mathrm{Pr}}C_1 + \mathrm{Pr})^2 \\ &\quad\times[C_1\overline{\mathrm{Pr}}(dC_2\overline{\mathrm{Pr}} + d\overline{\mathrm{Pr}} + 2) + \overline{\mathrm{Pr}}C_2(d\mathrm{Pr} - 1) \\ &\quad + \mathrm{Pr}(d\overline{\mathrm{Pr}} + 1)] - a^2F_0^2\mathrm{Pr}^{-2}\overline{\mathrm{Pr}}^2(\mathrm{Pr}+\overline{\mathrm{Pr}}C_2)\}, \end{aligned} \tag{42}$$

$$C_4(\beta) = \frac{1}{\mathrm{Pr} + C_1\overline{\mathrm{Pr}}}, \tag{43}$$

$$C_5(\beta) = \frac{1}{\mathrm{Pr} + C_2\overline{\mathrm{Pr}}}, \tag{44}$$

$$C_6(\beta) = \frac{F_0\mathrm{Pr}^{-1}\overline{\mathrm{Pr}}}{\mathrm{Pr} + C_1\overline{\mathrm{Pr}}}a\,. \tag{45}$$

The corresponding BGK results can be obtained from Eqs. (34)–(45) by taking Pr= 1.

When $a = 0$, one has $F_\eta = F_\kappa = 1$ and $\Phi = 0$, so that the NS results are reobtained. In the limit of small shear rates one gets

$$F_\eta = 1 - \frac{6\mathrm{Pr}^{-1}(1 + 2\mathrm{Pr})}{2+d}a^2 + \mathcal{O}(a^4), \tag{46}$$

$$\begin{aligned} F_\kappa &= 1 - \mathrm{Pr}^{-2}[\mathrm{Pr}^2(20 + 4d) + \mathrm{Pr}(104 + 22d) \\ &\quad - 16 - 8d](2+d)^{-2}a^2 + \mathcal{O}(a^4), \end{aligned} \tag{47}$$

$$\Phi = -\mathrm{Pr}^{-1}\frac{(4+d)(\mathrm{Pr}+1)}{2+d} + \mathcal{O}(a^2). \tag{48}$$

Apart from obtaining the nonlinear transport coefficients, the use of a kinetic model allows one to explicitly get the velocity distribution function $f(\mathbf{r},\mathbf{v})$. The distribution function can be written as $f(\mathbf{r},\mathbf{v}) = n(m/2\pi k_B T)^{d/2}\,\Psi(\boldsymbol{\xi})$, where $\Psi(\boldsymbol{\xi})$ is given by the expression [9]

$$\Psi(\boldsymbol{\xi}) = \frac{2\delta(1+\delta)^{d/2}}{\mathrm{Pr}^{-1}\epsilon|\xi_y|}(C_3C_4)^{-1/2}C_5^{1-\frac{d}{2}}\int_{t_0}^{t_1}dt\,[2t - (1-\delta)t^2]^{-(1+\frac{d}{2})}\exp\left(-\frac{2\delta}{1+\delta}\frac{1-t}{\mathrm{Pr}^{-1}\epsilon\xi_y}\right) \times\exp\left\{-\frac{1+\delta}{2t-(1-\delta)t^2}\left[C_3^{-1}\left(\xi_x+\frac{2a\delta}{1+\delta}\times\frac{1-t}{\epsilon}\right)^2\left(C_4^{-1}+C_6^2C_3^{-1}\right)\xi_y^2+\frac{d-2}{C_5}\xi_z^2 +2C_6C_3^{-1}\xi_y\left(\xi_x+\frac{2a\delta}{1+\delta}\frac{1-t}{\epsilon}\right)\right]\right\}. \quad (49)$$

Here, $(t_0,t_1)\equiv(0,1)$ if $\xi_y>0$ and $(t_0,t_1)\equiv[1,2/(1-\delta)]$ if $\xi_y<0$. Furthermore, $\boldsymbol{\xi}=(m/2k_BT)^{1/2}\mathbf{V}$,

$$\delta = \frac{\epsilon}{(\epsilon^2+8\gamma)^{1/2}}, \quad (50)$$

and

$$\epsilon = \left(\frac{2k_B}{mT}\right)^{1/2}\frac{1}{\zeta}\frac{\partial T}{\partial y} \quad (51)$$

is a reduced local thermal gradient. The nonlinear dependence of $\Psi(\boldsymbol{\xi})$ on the dimensionless gradients a and ϵ is very apparent.

4 COMPARISON WITH MD SIMULATIONS

As mentioned in the Introduction, Risso and Cordero [4] have performed computer MD experiments to analyze the shear-rate dependence of the generalized transport coefficients for a hard disk gas ($d=2$). In their MD simulations a system of hard disks is enclosed inside a square box and the vertical walls (along the y direction) are treated as periodic boundaries. When a particle collides with a horizontal wall, its velocity is replaced by one randomly chosen from the local equilibrium velocity distribution function characterized by the hydrodynamic fields imposed in this boundary. In this section we compare their simulation data with the theoretical results derived from Grad's method of the BE and from the kinetic models. This comparison will be useful to assess the reliability of the different approaches.

Figures 1–3 show the shear-rate dependence of F_η, F_κ and Φ, respectively, as obtained from MD simulations, from Grad's method, and from the ES and BGK models. The nonlinear (reduced) shear viscosity F_η (Fig. 1)

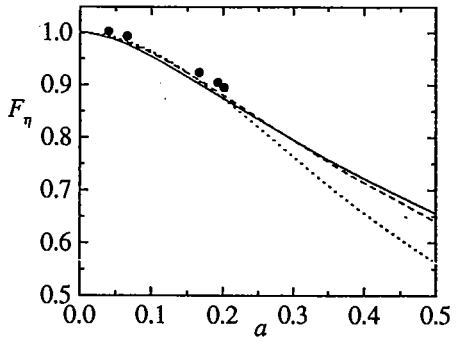

Figure 1: Plot of the viscosity function F_η versus the reduced shear rate a for a hard disk gas as obtained from MD simulation (circles), from the ES model (solid line), from Grad's method (dotted line), and from the BGK model (dashed line).

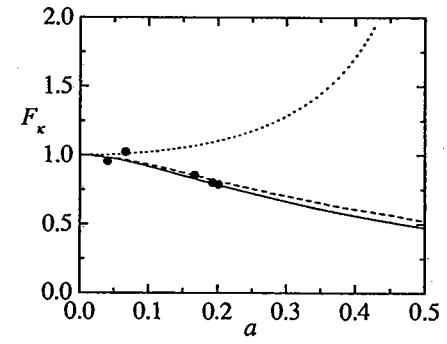

Figure 2: Same as in Fig. 1, but for the thermal conductivity function F_κ.

is probably the most relevant transport coefficient of the problem. We observe that the qualitative trends predicted by all the approximations are confirmed by the simulation data, namely, the viscosity decreases as the shear rate increases (shear thinning effect). At a quantitative level, the discrepancies observed for this coefficient between the theories and the simulation are smaller than 3%. Figure 2 shows the behavior of the thermal conductivity coefficient. In this case is evident that Grad's solution fails to capture the shear-rate dependence of F_κ. This disagreement could be anticipated from the comparison with the perturbation solution of the BE for Maxwell

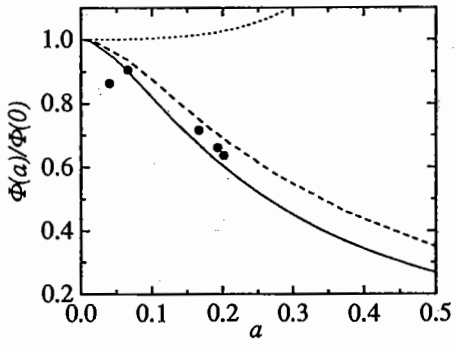

Figure 3: Same as in Fig. 1, but for the cross coefficient $\Phi(a)$, relative to the Burnett value $\Phi(0)$.

molecules in the 3D case. On the other hand, the ES and BGK models fit quite well the MD data, the discrepancies being smaller than 1% in the case of the ES model. As it can be observed in Fig. 3, the kinetic models are again clearly superior over Grad's approximation in predicting the shear-rate dependence of Φ. Thus, for instance at $a \simeq 0.2$, the kinetic models lead to a relative error smaller than 9%. Although Grad's theory provides the exact asymptotic value $\Phi(0)$, its predictions worsen as the system goes away from equilibrium.

Needless to say, the BE is only valid in the zero density limit. Nevertheless, in a MD experiment one has to fix a nonzero (but very small) average density, which is related to the ratio of the number of simulated particles to the area of the system. As a consequence, the collisional contributions to the transport coefficients are not *strictly* zero. Therefore, the BE cannot exactly reproduce the simulation data, although the discrepancies between both can be neglected as the density becomes very small. In the simulations of Ref. [4] the disks covered 1% of the system area, so that the corrections to the equation of state due to density effects are less than 2%. This slight discrepancy can be avoided using the Monte Carlo simulation method. In addition, it is important to keep in mind that boundary effects cannot be completely eliminated in the simulations, and so there exist velocity slips and temperature jumps near the horizontal walls. As a consequence, the bulk region (where the nonlinear transport coefficients are computed) becomes smaller as the shear rate increases. This is the reason for which the MD simulations performed in Ref. [4] are restricted to a range of shear rates where non-Newtonian effects are hardly significant. Thus, in order to state clearly what of the analytical approximations is superior, we have to extend the range of values of a considered in the MD simulations. To overcome all the above drawbacks, we have recently used the DSMC method to numerically solve the BE in the steady planar Couette flow for Maxwell molecules and hard spheres [11].

5 MONTE CARLO SIMULATION: BOUNDARY CONDITIONS

In this Section, we briefly describe the Direct Simulation Monte Carlo (DSMC) method [10] as well as its application to the planar Couette flow problem [11].

In the DSMC method [10], the velocity distribution function is represented by the velocities and positions of a sufficiently large number of particles. Given the geometry of the problem, the physical system is split into layers of width sufficiently smaller than the mean free path. The velocities and coordinates are updated in two stages (streaming and collisions) that are decoupled at each time step. The time step is much smaller than the mean free time. In the *streaming stage*, the particles are moved ballistically, and those particles crossing the boundaries are reentered with velocities sampled from the corresponding probability distribution. The *collision stage* proceeds following certain stochastic rules which depend on the interaction potential considered. The algorithm captures the dynamics associated to the BE, preserving properties such as the molecular chaos (*stosszahlansatz*). Starting from an equilibrium initial state, the system evolves driven by the boundary conditions. After a transient period, the system reaches a steady state. In the course of the simulations, local values of the hydrodynamic fields and of the fluxes are computed averaging the corresponding microscopic quantities over the particles inside the layer. From these averages one can get local values of the gradients and of the transport coefficients.

In the DSMC simulations, nonequilibrium boundary conditions have been employed to diminish the influence of finite-size effects [11]. We now describe these new boundary conditions and the differences between them and the standard ones. In order to be concrete, we will focus on the 3D-system case. As said before, the simulated gas is enclosed between two parallel plates located at $y = 0$ and $y = L$. The plates are moving along the x-direction with velocities $\mathbf{U}_0 = U_0\widehat{\mathbf{x}}$ and $\mathbf{U}_L = U_L\widehat{\mathbf{x}}$, respectively. In addition, they are kept at temperatures T_0 and T_L, respectively. The corresponding boundary conditions can be characterized by the kernels $K_{0,L}(\mathbf{v}, \mathbf{v}')$ defined as follows. When a particle with velocity $\mathbf{v}'$ hits

the wall at $y = L$, the probability of being remitted with a velocity $\mathbf{v}$ within the range $d\mathbf{v}$ is $K_L(\mathbf{v},\mathbf{v}')d\mathbf{v}$; the kernel $K_0(\mathbf{v},\mathbf{v}')$ represents the same but at $y = 0$. The boundary conditions are then [13]

$$\Theta(\pm v_y)\ |v_y|f(y=\{0,L\},\mathbf{v}) = \Theta(\pm v_y)\int d\mathbf{v}'\,|v_y'| \times K_{0,L}(\mathbf{v},\mathbf{v}')\Theta(\mp v_y')f(y=\{0,L\},\mathbf{v}',t). \tag{52}$$

In the case of complete accommodation with the walls, $K_{0,L}(\mathbf{v},\mathbf{v}') = K_{0,L}(\mathbf{v})$ does not depend on the incoming velocity $\mathbf{v}'$ and can be written as

$$K_{0,L}(\mathbf{v}) = A_{0,L}^{-1}\Theta(\pm v_y)|v_y|\phi_{0,L}(\mathbf{v}), \tag{53}$$

$$A_{0,L} = \int d\mathbf{v}\,\Theta(\pm v_y)|v_y|\phi_{0,L}(\mathbf{v}). \tag{54}$$

The functions $\phi_{0,L}(\mathbf{v})$ can be interpreted as the probability distribution of a fictitious gas in contact with the system at $y = L$. Equations (53) and (54) mean that when a particle hits a wall, it is replaced by a particle leaving from the fictitious gas. Obviously, the functions $\phi_{0,L}(\mathbf{v})$ are consistent with the velocity and the temperature of the walls, i.e.,

$$U_{0,L} = \int d\mathbf{v}\,v_x\phi_{0,L}(\mathbf{v}), \tag{55}$$

$$k_BT_{0,L} = \frac{1}{3}m\int d\mathbf{v}\,(\mathbf{v}-\mathbf{U}_{0,L})^2\phi_{0,L}(\mathbf{v}). \tag{56}$$

The usual choice of $\phi_{0,L}(\mathbf{v})$ is that of a Maxwell-Boltzmann distribution:

$$\phi_{0,L}^{\mathrm{MB}}(\mathbf{v}) = \left(\frac{m}{2\pi k_BT_{0,L}}\right)^{3/2}\exp\left[-\frac{m(\mathbf{v}-\mathbf{U}_{0,L})^2}{2k_BT_{0,L}}\right]. \tag{57}$$

These boundary conditions were used in the MD simulations of Ref. [4]. In this case, the system is understood to be enclosed between two independent baths at *equilibrium*. This type of boundary condition is adequate if one is interested in studying realistic boundary effects [14], but not when one wants to measure transport properties in the bulk region.

Therefore, in order to inhibit the influence of boundary effects, an alternative type of boundary condition has been proposed [11, 15]. The idea is to imagine that the above two fictitious baths are in *nonequilibrium* states resembling the state of the actual gas near the walls. Since the distribution function of the actual gas is not known *a priori*, we assume that the fictitious gases are described by the distribution function given by the BGK approximation for the steady planar Couette flow, Eq. (49) for Pr=1 and $d = 3$. More specifically, this second type of boundary condition is

$$\begin{aligned}\phi_{0,L}^{\mathrm{BGK}}(\mathbf{v}) &= \pi^{-3/2}\frac{m}{k_BT_{0,L}}\frac{\alpha_{0,L}(1+\alpha_{0,L})^{3/2}}{\epsilon_{0,L}|v_y|}\\ &\times\int_{t_0}^{t_1}dt\,\left[2t-(1-\alpha_{0,L})t^2\right]^{-5/2}\\ &\times\exp\left\{-\left(\frac{2k_BT_{0,L}}{m}\right)^{1/2}\frac{2\alpha_{0,L}}{1+\alpha_{0,L}}\frac{1-t}{\epsilon_{0,L}v_y}\right.\\ &\left.-\frac{m}{2k_BT_{0,L}}\frac{1+\alpha_{0,L}}{2t-(1-\alpha_{0,L})t^2}\left[(v_x-U_{0,L}+\frac{2a'\alpha_{0,L}}{1+\alpha_{0,L}}\frac{1-t}{\epsilon_{0,L}}\right)^2+v_y^2+v_z^2\right]\right\},\end{aligned} \tag{58}$$

where $(t_0,t_1) = (0,1)$ if $v_y > 0$ and $(t_0,t_1) = [1,2/(1-\alpha_{0,L})]$ if $v_y < 0$, and $\alpha_{0,L} = \epsilon_{0,L}/[\epsilon_{0,L}^2 + 8\gamma_{\mathrm{BGK}}(a')]^{1/2}$. Here, a' is the *estimated* value of the reduced shear rate, as predicted by the BGK model for specific values of the boundary parameters $U_{0,L}$ and $T_{0,L}$. Moreover, $\gamma_{\mathrm{BGK}}(a')$ is obtained from Eq. (37) for Pr=1 and $d = 3$. Given the values of the four independent boundary parameters $U_{0,L}$ and $T_{0,L}$ (as well as the distance L), the shear rate a' and the local thermal gradients $\epsilon_{0,L}$ are fixed by the conditions (16)–(18). Therefore,

$$a' = \frac{U_L-U_0}{\mathcal{L}}, \tag{59}$$

$$\epsilon_{0,L} = \frac{1}{L}\left(\frac{2k_BT_{0,L}}{m}\right)^{1/2}\left[\frac{T_L-T_0}{T_{0,L}} \pm \frac{m\gamma_{\mathrm{BGK}}(a')\mathrm{Pr}}{k_BT_{0,L}}\mathcal{L}^2\right], \tag{60}$$

The quantity $\mathcal{L}$ is related to the actual separation L between the plates through the nonlinear equation

$$L = \int_0^{\mathcal{L}}\frac{ds}{\nu(s)}. \tag{61}$$

Here s is a variable in terms of which the temperature is a quadratic function. Given the values of the parameters $U_{0,L}$, $T_{0,L}$, and L, the values of the parameters a', $\epsilon_{0,L}$, and $\mathcal{L}$ can be obtained solving the nonlinear set of equations (59)–(61). The knowledge of these boundary parameters allows one to obtain the distributions $\phi_{0,L}^{\mathrm{BGK}}(\mathbf{v})$, according to Eq. (58).

The numerical algorithm described in this section has been successfully tested simulating the BGK equation by a DSMC-like method similar to the one described in Ref. [16]. Once the boundary conditions are correctly implemented and the simulation parameters are well chosen, the simulation results exhibit an excellent agreement with the theoretical BGK predictions, even at the level of the velocity distribution function [11].

6 COMPARISON WITH MONTE CARLO SIMULATIONS

We now display a comparison between the transport coefficients obtained from the DSMC simulation method and the (universal) theoretical predictions provided by Grad's method and the kinetic models. The simulations have been performed considering the Maxwell and hard-sphere interaction potentials [11] and the transport coefficients have been computed inside the bulk domain, i.e., the region of the system where boundary effects are negligible. However, in a simulation with a finite size of the system, it is not possible to avoid boundary effects completely. A way of diminishing these effects is to use the nonequilibrium boundary conditions based on the BGK distribution, Eq. (58), instead of the conventional equilibrium boundary conditions (57). This can be confirmed when one calculates the hydrodynamic profiles by means of the DSMC method and uses both type of boundary conditions. In the case of Maxwell molecules, the comparison between the simulations results and the (exact) solution (16)–(18) indeed shows that the velocity slips and the temperature jumps at the walls are much larger in the case of the equilibrium boundary conditions than in the case of the nonequilibrium ones [11]. Further, the pressure obtained with the BGK boundary conditions is practically constant, except near the upper plate, while the one obtained with the equilibrium conditions is only nearly constant in a small region around $y/L \simeq 0.75$ [11]. These results clearly indicate that the BGK boundary conditions are much more efficient than the equilibrium ones to measure transport properties in the bulk region. Therefore, in what follows we will only consider the BGK conditions. In each case, a bulk domain comprised between the layers $y = y_0$ and $y = y_1$ has been identified. In this region of the system, $a \simeq$ const, $p \simeq$ const, and $\gamma \simeq$ const, and averages of a, F_η, F_κ, and Φ have been taken over those layers. Typical values are $y_0/L \simeq 0.2$ and $y_1/L \simeq 0.8$.

Figure 4 shows the shear rate dependence of the nonlinear viscosity represented by the function $F_\eta(a)$. At a qualitatively level, the three theories predict correctly the behavior of the simulation data and show the shear thinning effect (the decrease of F_η with increasing a). On the other hand, the results obtained from the kinetic models (especially from the BGK model) are superior over Grad's predictions. It is also interesting to remark a slight influence of the interaction potential on the viscosity function $F(\eta)$. In Fig. 5, we plot the nonlinear thermal conductivity $F_\kappa(a)$. As it can be observed, Grad's solution does not capture the main trends of F_κ. This failure was already noted in the case of hard disks (cf. Fig. 2). Again,

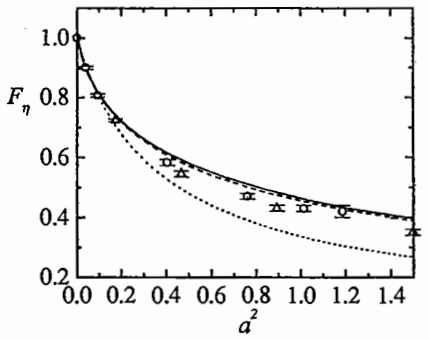

Figure 4: Plot of the the viscosity function F_η as a function of the shear rate. The symbols are simulation data for Maxwell molecules (circles) and for hard spheres (triangles), while the lines are the theoretical predictions given by the ES kinetic model (solid line), the BGK kinetic model (dashed line), and the Grad method (dotted line).

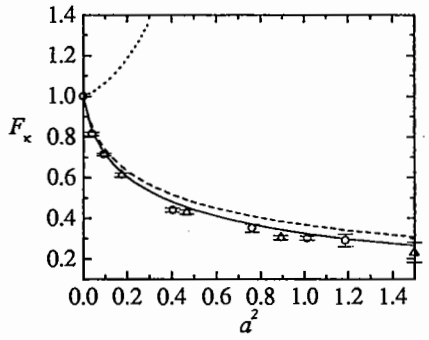

Figure 5: Same as in Fig. 4, but for the thermal conductivity function F_κ.

the kinetic models present a good agreement, especially in the case of the ES model. Finally, the shear rate dependence of the cross-coefficient Φ is displayed in Fig. 6. As it was already noted in the case of hard disks, Grad's method gives a wrong prediction while the kinetic models describe fairly well the nonlinear behavior of this function. In the case of the ES model, the agreement with the simulation data is practically perfect. In summary, the general conclusions anticipated from the comparison

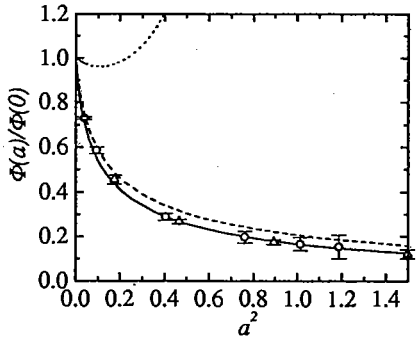

Figure 6: Same as in Fig. 4, but for the cross coefficient Φ, relative to the Burnett value $\Phi(0)$.

with MD data for a hard disk system and relatively small values of the shear rate, are confirmed by considering the DSMC results for a 3D-system of Maxwell molecules or hard spheres.

7 CONCLUDING REMARKS

In this review we have studied the steady planar Couette flow in a dilute gas under conditions for which the (linear) Navier-Stokes theory does not apply. In this state, there are two parameters measuring the departure of the system from equilibrium: the shear rate a and the thermal gradient ϵ. Our goal has been to determine the momentum and heat fluxes in terms of the nonequilibrium parameters a and ϵ. These fluxes are mainly characterized by three shear-rate dependent generalized transport coefficients: a viscosity function F_η, a thermal conductivity function F_κ, and a cross coefficient Φ. In the non-Newtonian regime (not small values of the shear rate a), these transport coefficients are highly nonlinear functions of a.

The natural framework to determine such a nonlinear dependence is the Boltzmann equation. However, due to the intricacy of the Boltzmann collision operator, an exact solution of the Boltzmann equation in the Couette flow problem is not known. This leads to use alternative approaches, such as the Grad method and/or kinetic models (the BGK and ES models) or on the computational side, molecular dynamics and/or Monte Carlo simulations. The comparison between the simulation and theory can be considered as an stringent test to assess the reliability of the above analytic methods to compute nonlinear transport properties. In addition, since we are interested in transport phenomena occurring in the bulk region, we have also devised a new "nonequilibrium" boundary condition to inhibit the influence of finite-size effects in the DSMC simulations. This boundary condition is based on the actual distribution function of the BGK model in the Couette flow state.

The comparison with the theoretical predictions shows that the kinetic models provide a reliable description of the generalized transport coefficients, even for large values of the shear rate. With respect to the Grad method, it essentially captures the shear-rate dependence of the nonlinear shear viscosity but it dramatically fails for the coefficients measuring the heat flux. This is basically due to the truncation scheme of the Grad method at the level of the heat flux, in contrast to what happens in the kinetic models where all the velocity moments are taken into account. On the other hand, in the ES model the reference distribution function appearing in the collision term is an anisotropic Gaussian parametrized by the pressure tensor. This choice yields the correct Prandtl number $\mathrm{Pr} = 1 - 1/d$. In the BGK model, the reference distribution is that of the local equilibrium and the model gives the incorrect Prandtl number Pr=1. The agreement with the Monte Carlo simulations of the ES model is generally better than the BGK model, especially in the heat flux. This fact can justify the use of kinetic models more sophisticated than the BGK model (such as the ES model) in the Couette problem, at the expense of the simplicity of the model. Nevertheless, this conclusion cannot be extended to other nonequilibrium situations where the Prandtl number does not play an important role [17]. Another important outcome of the simulation results is that the shear-rate dependence of the transport coefficients is hardly sensitive to the interaction potential when one scales conveniently the quantities. This conclusion agrees with the predictions of the kinetic models where (in appropriate reduced units) their results are universal, independent of the interaction law considered.

In summary, it appears that many interesting questions regarding nonlinear transport phenomena may be addressed by means of the BGK and ES kinetic models. The results obtained here in the Couette flow problem support this assertion. On the other hand, it must be noted that any extension of the conclusions reported here to dense fluids must be taken with caution, since the collision transfer mechanism is absent in the low-density regime. However, a qualitative good agreement with simulations could be obtained when one introduces convenient nondimensional variables. Comparisons carried out in the uniform shear flow problem support this expectation [18].

Partial support from the DGES (Spain) through Grant No. PB97-1501 and from the Junta de Extremadura (Fondo Social Europeo) through Grant No. IPR99C031 is acknowledged.

REFERENCES

[1] Cercignani, C. 1990, Mathematical Methods in Kinetic Theory, Plenum Press, New York.

[2] Chapman, S. and Cowling, T. G. 1970, The Mathematical Theory of Nonuniform Gases, Cambridge University Press, Cambridge.

[3] Tij, M. and Santos, A. 1995, Phys. Fluids, 7, 2858.

[4] Risso, D. and Cordero, P. 1997, Phys. Rev. E, 56, 489; 1998, Phys. Rev. E, 57, 7365 (Erratum).

[5] Brey, J. J., Santos, A. and Dufty, J. W. 1987, Phys. Rev. A, 36, 2842.

[6] Kim, C. S., Dufty, J. W., Santos, A. and Brey, J. J. 1989, Phys. Rev. A, 40, 7165.

[7] Garzó, V. and López de Haro, M. 1994, Phys. Fluids, 6, 3787.

[8] Garzó, V. and López de Haro, M. 1997, Phys. Fluids, 9, 776.

[9] Montanero, J. M. and Garzó, V. 1998, Phys. Rev. E, 58, 1836.

[10] Bird, G. A. 1994, Molecular Gas Dynamics and the Direct Simulation of Gas Flows, Clarendon, Oxford.

[11] Montanero, J. M., Santos, A. and Garzó, V. 2000, Phys. Fluids, 12, 3060.

[12] McLennan, J. A. 1989, Introduction to Nonequilibrium Statistical Mechanics, Prentice-Hall, Englewood Cliffs, New York.

[13] Dorfman, J. R. and van Beijeren, H. 1977, Statistical Mechanics, Part B, B. J. Berne (Ed.), Plenum, New York, 65.

[14] Wadsworth, D. C. 1993, Phys. Fluids A, 5, 1831.

[15] Montanero, J. M., Alaoui, M., Santos, A. and Garzó, V. 1994, Phys. Rev. E, 49, 367.

[16] Montanero, J. M., Santos, A., Lee, M., Dufty, J. W. and Lutsko, J. F. 1998, Phys. Rev. E, 57, 546.

[17] Garzó, V. 1997, Physica A, 243, 113.

[18] Naitoh, T. and Ono, S. 1979, J. Chem. Phys., 70, 4515; Zwanzig, R. 1979, J. Chem. Phys., 71, 4416.